Structural-Functional Relationships of the Dynein, Spokes, and Central-Pair Projections Predicted from an Analysis of the Forces Acting within a Flagellum

Charles B. Lindemann
Department of Biological Sciences, Oakland University, Rochester, Michigan

ABSTRACT In the axoneme of eukaryotic flagella the dynein motor proteins form crossbridges between the outer doublet microtubules. These motor proteins generate force that accumulates as linear tension, or compression, on the doublets. When tension or compression is present on a curved microtubule, a force per unit length develops in the plane of bending and is transverse to the long axis of the microtubule. This transverse force (t-force) is evaluated here using available experimental evidence from sea urchin sperm and bull sperm. At or near the switch point for beat reversal, the t-force is in the range of 0.25–1.0 nN/μm, with 0.5 nN/μm the most likely value. This is the case in both beating and arrested bull sperm and in beating sea urchin sperm. The total force that can be generated (or resisted) by all the dyneins on one micron of outer doublet is also $\sim$0.5 nN. The equivalence of the maximum dynein force/μm and t-force/μm at the switch point may have important consequences. Firstly, the t-force acting on the doublets near the switch point of the flagellar beat is sufficiently strong that it could terminate the action of the dyneins directly by strongly favoring the detached state and precipitating a cascade of detachment from the adjacent doublet. Secondly, after dynein release occurs, the radial spokes and central-pair apparatus are the structures that must carry the t-force. The spokes attached to the central-pair projections will bear most of the load. The central-pair projections are well-positioned for this role, and they are suitably configured to regulate the amount of axoneme distortion that occurs during switching. However, to fulfill this role without preventing flagellar bend formation, moveable attachments that behave like processive motor proteins must mediate the attachment between the spoke heads and the central-pair structure.

INTRODUCTION

The flagellum is a biological machine that is a self-contained mechanochemical oscillator and a force-producing organelle of motility. Therefore, to fully understand the events involved in the beat cycle, it is crucial to know how forces are produced and distributed within the axoneme. The Geometric Clutch hypothesis (Lindemann, 1994a) proposes that the transverse forces (t-forces) that act on the outer doublet microtubules regulate the activity of dynein to produce the flagellar beat cycle. In this view, the t-force can push the doublets together facilitating the engagement of the dyneins, or pry the doublets apart resulting in a termination of motor function. The absolute magnitude of the t-force increases in proportion to the curvature of the flagellum and the longitudinal tension on the doublets. Therefore, as a bend develops the magnitude of the t-force becomes progressively larger, prying the doublets apart and leading to the termination of dynein motor activity on the active side of the flagellum. Computed models based on this principle have shown that using the t-force to regulate dynein switching can simulate the beating of flagella and cilia with lifelike results (Lindemann, 1994b, 2002). The same model, when adapted to a bull sperm flagellum, simulates the beating of the sperm flagella and accurately predicts experimentally observed arrest behaviors (Lindemann, 1996; Holcomb-Wygle et al., 1999).

Data output from the computed model suggests an interesting relationship between the t-force and the dynein force per head. When the model is scaled to give a good simulation of ciliary or flagellar motility, the t-force that develops per micron of length when the dyneins switch ''off,'' is larger than the sum of the force developed by the dyneins in the same one micron length of flagellum. This suggested the possibility that the t-force may be able to act directly to overcome and inactivate the dyneins at the point of beat reversal.

The objective of this report is to examine the forces that are acting within the axoneme directly and see if the relationship predicted by the model is feasible. Toward this goal the magnitude of the dynein force and the t-force at the switch point is evaluated in real flagella of sea urchin and bull sperm. In addition, the consequences of the internal force balance, with regard to the structure-function relationship of axonemal components, are evaluated.

The sliding doublet mechanism is accepted as the basis of flagellar bend formation (Satir, 1979). In this study, the sliding doublet mechanism will serve as the basis for the analysis of force redistribution within the axoneme. The available information on the forces acting in real flagella, near the point of beat reversal, are presented to demonstrate the relevance of force transmission within the axoneme to dynein-bridge switching. The role of individual axoneme components in managing the stresses within the axoneme is examined. An attempt is made to identify structural and functional requirements that must be met by specific

Submitted September 19, 2002, and accepted for publication February 6, 2003.

Address reprint requests to Charles B. Lindemann, Dept. of Biological Sciences, Oakland University, Rochester, MI 48309-4476. Tel.: 248-370-3576; E-mail: lindeman@oakland.edu.

0006-3495/03/06/4115/12 $2.00

components of the axoneme. Finally, several consequences and predictions that follow from the analysis will be presented, including a novel role for the spokes and central-pair projections.

The dynein force

How much force does dynein produce and how much force can a dynein resist? There are a number of measurements available on the force that is produced by an isolated dynein. The experimentally determined values are in the range of 2–5 pN per dynein head (Ashkin et al., 1990, Shingyoji et al., 1998; Sakakibara et al., 1999; Hirakawa et al., 2000). The high-end value of 5 pN per dynein head is in good agreement with the two estimates of the force that can be produced per dynein head in an intact flagellum (Yoneda, 1960; Schmitz et al., 2000). An isometric stalling force of 5 pN/dynein head yields a good experimental fit between modeled flagella (Brokaw, 1999b), modeled cilia (Lindemann, 2002), and the behavior of real flagella and cilia. Therefore, within a factor of two, the force per dynein head does not appear to be in doubt and is, at maximum, 5 pN/ head.

The number of dynein heads per micron of length in a cilium or a flagellum is well-established. In *Chlamydomonas* there are 73 inner arm dynein heads and 125 outer arm dyneins per micron, for a total of 198 dynein heads/μm (Piperno and Luck, 1982). If we assume all dyneins can contribute the maximum force per head, then the dyneins in one micron of flagellum can pull with a maximum force of 990 pN or approximately 1.0 nN/μm.

THE T-FORCE

Estimated from sea urchin sperm

The active dyneins in a beating flagellum contribute the force to bend the flagellum. The tension and compression on the doublets that result from the action of the individual dynein motors bends the flagellum by producing torque acting between the doublets. The polarity of the nine outer doublet microtubules is uniform, therefore the minus-end-directed dyneins maintain the same sliding direction around the ring of nine outer doublets (Sale and Satir, 1977). The dyneins of each doublet propel their own doublet baseward, while pushing the next higher numbered doublet tipward. Sea urchin sperm flagella and most other flagella exhibit a relatively planar beat. To bend the flagellum into planar waves of bending, the dyneins on doublets numbered 1–4 must alternate their action with the dyneins on doublets 6–9. The serial arrangement of the doublets on the two sides of the axoneme will transfer all or most of the resultant longitudinal force to the most widely spaced doublets that are actively participating in the sliding episode, as illustrated in Fig. 1. This means that, typically, doublets numbered 1 and 5–6 in the standard numbering system will carry most of the resulting tension or compression. Each of the intervening doublets (7–9 in the diagram) is being pulled tipward by the dyneins on its lower numbered neighbor and baseward by its own dyneins. This serves to cancel the tension and compression on the doublets that interconnect and to transfer the net force to the elements at the beginning and end of the active series. Due to the serial arrangement, the total tension or compression that the first and last doublets (1 and 5–6) experience is approximately equal to the magnitude of tension or compression generated by the force output of the dyneins on one doublet. Therefore, we can find the maximum magnitude of the tension-compression force couple by the sum of the force output of the dyneins on a single doublet.

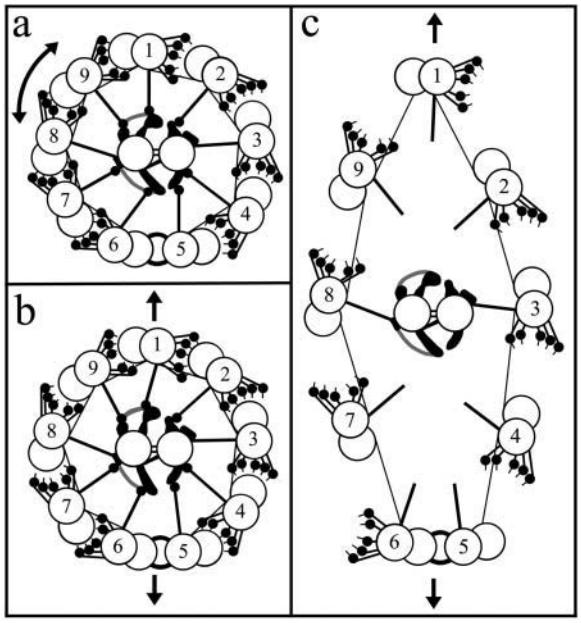

FIGURE 1 Force transfer in the flagellar axoneme. (*a*) The proposed configuration of the axoneme during the active formation of a new bend. The dyneins on the left side of the axoneme (doublets 6–9) are engaged and pulling, whereas those on the opposite side (doublets 1–4) are inactive. The force from each engaged set of dyneins is relayed to the first and last outer doublet in the active group as indicated by the doubleheaded arrow, in this case doublets 1 and 5–6. In the case illustrated, doublet 1 is pulled tipward and is under tension, whereas the 5–6 complex is pushed baseward and is under compression. (*b*) When a bend has formed and reached the critical curvature for switching, the t-force becomes large enough to disengage the dyneins on the active side as illustrated. At this crucial instant the t-force is transferred to the spokes and central-pair projections as indicated by the outwardly directed arrows. The central-pair projections not only flex outward bearing the t-force, but also limit the distortion of the axoneme. The increased spacing of the doublets on the active side, coupled with the restraining action of the spoke and central-pair projections, makes it possible for dynein arms on the inactive side to begin to engage. (*c*) This illustration shows the putative condition of *Chlamydomonas* spoke-head deficient mutants. In the absence of the spoke heads, the nexin links bear the full t-force, exerted in the direction of the arrows, as the dyneins on the active side disengage. Based on estimates of nexin elasticity (see text), the t-force causes a major distortion of the axoneme preventing reengagement of dyneins on either side of the axoneme. This interrupts the beat cycle until the t-force diminishes sufficiently to allow reengagement.

The tension and compression on these doublets also creates a force component acting transverse to the axis of the doublet whenever there is a bend present on the flagellum. This force, acting transverse to the axis of the doublets, is referred to as the t-force.

In several earlier reports the t-force has been analyzed and considered as a potential regulator of dynein function (Lindemann, 1994a,b; Lindemann and Kanous, 1997). A computer model based on this concept, called the Geometric Clutch, can simulate the beating of cilia and flagella. The t-force acting on the doublets of the axoneme is a sum of two components. One component is produced locally by stretching the interdoublet connections and the second global component is due to the tension on the doublets and the curvature of the flagellum (see Lindemann, 1994a, for an analysis of the two components). Both of these components have been calculated in the computed model, for both are tractable to geometric analysis. The global component is always in the plane defined by the local curvature, which for a planar waveform means it is aligned with the plane of bending. It is also the larger component of the t-force. In a beating flagellum the global component is $\sim$100$\times$ larger than the local component when switching occurs, as is presented in detail in the section on the switching mechanism. The global component of the t-force is simply the product of the longitudinal tension (or compression) on each doublet multiplied by the local curvature:

$$t\text{-}force = longitudinal\,force \times curvature. \quad (1)$$

The radius of curvature that develops just before a newly formed bend begins to propagate along a sea urchin flagellum was found from micrographs of free-swimming sea urchin sperm, as illustrated in Fig. 2 *a*. The bends that develop in the proximal portion of flagellum have an average radius of curvature of $\sim$4 μm and therefore 2.6×10^5 radians/m is the curvature of the bend. These averages were obtained from seven measurements on micrographs published by Gibbons and Gibbons (1972) and Brokaw (1965, 1990). The compiled data together with the source is displayed in Table 1. The bends selected were the most fully developed proximal bend just before it begins to travel down the flagellum. The interbend distance, shown in Fig. 2 *a*, is the length of flagellum where the curvature is visibly changing and therefore the dyneins are pulling to form the proximal bend. This distance was also measured from images of real beating flagella, and averaged 9 μm. In that length of flagellum, there are 1800 dynein heads on each doublet. If they are all pulling with the same 5 pN force/head, the cumulative tension is 9.0×10^{-9} N on the doublet they are pulling tipward, balanced by an equal and opposite compression on the doublet they are pushing baseward. Applying these values for the tension and curvature in Eq. 1 to get an estimate of the t-force yields 2.3×10^{-9} N/μm, or $\sim$2 nN/μm—which is a force *double* the force that the dynein in 1 μm of flagellum can sustain.

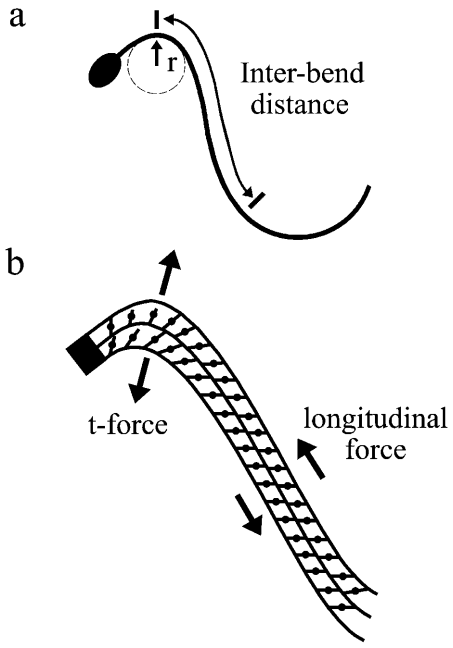

FIGURE 2 The balance of t-force and dynein bearing force in the axoneme. (*a*) A beating sperm flagellum is illustrated showing the method of finding the radius of curvature (*r*) for a newly formed bend. The length of flagellum that is contributing to the formation of the bend (interbend distance) is indicated and is the segment where the curvature is actively changing. It starts at the end of the circularly curved portion of the previous bend and extends to the crest of the new bend. (*b*) In a simplified representation of the forces acting in the bend, the contributing interbend dyneins push and pull on the doublets to create linear tension and compression. Arrows indicate the tension that develops on the concave side of the bend and the compression that develops on the convex side. In the curved bend, tension and compression lead to the development of outwardly directed t-force, as indicated by the paired arrows. The t-force that develops in the fully formed bend is equal to, or greater than, the holding capacity of the dyneins in the region of maximal curvature.

Fig. 2 *b* illustrates the essential concept, that the dyneins pulling in the interbend segment contribute linear force sufficient to generate a t-force that overpowers the dyneins in the bend.

Estimated from swimming bull sperm

In a major departure from the simple flagellum of sea urchin sperm, we shall consider the flagellum of the bull sperm. The outer dense fibers and sheath that surround the axoneme make these flagella much stiffer than those of sea urchins and simple cilia. Experimental estimates and theoretical estimates yield relative agreement that these flagella are more than 20$\times$ as stiff as the flagellum of a sea urchin sperm (Lindemann et al., 1973; Holcomb-Wygle et al., 2001). Mammalian sperm are very stiff and also quite large (a bull sperm flagellum is typically 60 μm in length). The waves produced are very long and the bends much less strongly curved than in a sea urchin sperm. Curvatures and interbend distances for swimming bull sperm, using the same method

TABLE 1 Proximal bend and interbend distance of sea urchin sperm and bull sperm

	Species	Bend type*	Curvature ($\times 10^5$ radians/m)	Interbend distance (μm)	Reference
Sea urchin					
Intact	*Strongylocentrotus purpuratus*	*P*	2.4	10	Brokaw, 1990
Reactivated (80 μM ATP)	*Lytechinus pictus*	*P*	3.0	6.2	Brokaw, 1990
Reactivated (80 μM ATP)	*Lytechinus pictus*	*R*	2.4	7.2	Brokaw, 1990
Intact	*Chaetopterus variopedatus*	*R*	2.7	8.3	Brokaw, 1965
Intact	*Colobocentrotus atratus*	*P*	2.5	9.4	Gibbons and Gibbons, 1972
Intact	*Colobocentrotus atratus*	*R*	2.0	14	Gibbons and Gibbons, 1972
Reactivated (1 mM ATP)	*Colobocentrotus atratus*	*R*	3.1	7.2	Gibbons and Gibbons, 1972
		$n = 7$	mean = 2.6 ± 0.38	mean = 8.9 ± 2.6†	
Bull sperm					
Intact	*Bos taurus*	*P*	1.2	23	Lindemann, this article
Intact	*Bos taurus*	*R*	0.86	25	Lindemann, this article
Reactivated (1 mM ATP)	*Bos taurus*	*P*	1.3	19	Lindemann, this article
Reactivated (1 mM ATP)	*Bos taurus*	*R*	0.72	22	Lindemann, this article
		$n = 4$	mean = 1.0 ± 0.27	mean = 22 ± 2.5‡	

*P = principal; R = reverse.
†Mean curvature × mean interbend distance = 23 ± 3.5.
‡Mean curvature × mean interbend distance = 22 ± 5.1.

that was used to collect the sea urchin data, are also given in Table 1. The curvature of a bend as it forms on the proximal region (at 20 μm) of a bull sperm flagellum averages 1.0×10^5 radians/m, whereas 22 μm is the interbend distance. Therefore, ~4400 dyneins pull together to produce a total longitudinal force of 22 nN on the doublets. Solving for the t-force using Eq. 1 yields 2.2×10^{-9} N/μm or $\approx$ 2 nN/μm, again.

Therefore, in a sperm at least 20× stiffer, twice as long, and operating at less than one-third of the beat frequency of a sea urchin sperm, the same number falls out as the first-order approximation of the t-force. The number is also double the total bearing force of the dyneins in a micron length of axoneme.

Finer tuning: force-velocity effects

The calculations provided thus far are simplified, and therefore only serve as first approximations of the stress dynamics in a real flagellum. There are some major factors that were not considered in the initial calculations that are important and must be addressed. In a swimming sperm, the microtubules are actively sliding. Dyneins, like all motor proteins, exhibit a force-velocity relation, and this trait will reduce the linear force developed in a moving flagellum. The point at which the bend reaches maximum curvature is near the point of sliding direction reversal. At that point the shear velocity (i.e., sliding velocity) is close to zero. The dynein in that region will generate close to the maximum force per dynein head. Farther away from the crest of each wave, the sliding velocity will be greater, reducing the force contributed by dynein. The average shear velocity for a reactivated sea urchin flagellum is 100 rad/s, as computed by Brokaw (1999a). The average interdoublet spacing in the plane of the beat is 42 nm. This, multiplied by the shear velocity, yields a mean sliding velocity of 4.2 μm/s for the entire contributing length.

How to correct for the force-velocity relationship of dynein still presents a bit of a dilemma. The force-velocity relationship for axonemal dynein was measured in disintegrating axonemes (Kamimura and Takahashi, 1981; Oiwa and Takahashi, 1988). If the force-velocity behavior measured by Oiwa and Takahashi (1988) is correct, then there is only a factor of 0.8 reduction in the linear force and hence the t-force. This would leave the t-force/μm at 1.6 nN/μm, still nearly twice the maximum dynein force. A model presented by Brokaw (1999b) based on a conventional four-state crossbridge cycle gives an excellent fit to the movements of a sea urchin flagellum. The force-velocity profiles computed by Brokaw (1999b, Fig. 11) to obtain the best fit to the experimental data would reduce the force per head to somewhere in the range of 1.0 to 1.25 pN per dynein head. If a correction based on Brokaw's analysis is factored into the calculation, then the linear force contributed by the dyneins is reduced to one-fourth of the original estimate, and the t-force to 0.5 nN/μm, due to the effect of sliding rate.

However, to be fully consistent with Brokaw's analysis, the differential functioning of inner and outer arm dyneins must be considered. The outer dynein arms are designed to contribute more force when the sliding rate is greater, acting as energy boosters (Brokaw and Kamiya, 1987; Brokaw, 1994). Therefore, they contribute maximally in the interbend regions where sliding is occurring, but much less in the regions where shear rate is near zero. Brokaw (1999b) found

that to obtain a best fit to experimental data, the outer arm dyneins must have a stalling-force at zero shear velocity of ~1 pN per head. When this is taken into account in a sea urchin flagellum, where slightly more than half of the dyneins are outer arm dyneins (a ratio of 8:7 outer to inner), the total force that the stalled dyneins can contribute is reduced to about one-half of the original estimate (0.5 nN/μm).

In this more complete view of the force balance, both the t-force/μm and the holding force of the dyneins/μm are reduced, and the net effect is that they become nearly equal. The t-force is adjusted downward to one-quarter of the original estimate and total dynein stalling force is adjusted downward to about one-half in the more sophisticated estimate. The consequence is that now the balance is 0.5 nN of t-force/μm $\approx$ 0.5 nN of dynein force/μm. In other words, switching occurs when the two are approximately equal.

It should be noted that this outcome is based on the most radical adjustment for the force-velocity behavior. If we assume instead that the measurements of Oiwa and Takahashi (1988) are a better representation of the true behavior of dynein in situ, then there is minimal correction to the original calculation. Thus, we may safely conclude that the t-force/μm is equal to, or greater than, the maximum summated force generated by the dyneins in a micron of flagellum.

Do all the dynein heads pull?

The calculations used above for sea urchin and bull sperm also assume that all the dynein arms contribute force. This may be an incorrect assumption. However, the force measurements on an intact bull sperm flagellum (Schmitz et al., 2000) and an intact compound cilium (Yoneda, 1960) suggest that all the dyneins may well pull, at least when the flagellum is pushing against an immovable load (isometric conditions). Schmitz et al. (2000) show that to explain the magnitude of the measured torque in real flagella or cilia, all of the dyneins in the stalled portion of the flagellum must pull with a force of ~5 pN/head. If this represents the average force of thousands of dyneins stalled at various positions in the power stroke, then it is likely that this force, times the step distance, represents the maximum work output of the dynein crossbridge cycle. Data from laser trap studies of isolated dyneins gives us a dynein step excursion distance of 8 nm (Hirakawa et al., 2000); therefore, the maximum work output per bridge cycle would be $\approx 4.0 \times 10^{-20}$ Joule. A typical value for the available energy from ATP in a living cell under physiological conditions is $\approx$46 kJ/mole. Expressed in terms of single molecular events, this equates to 7.6×10^{-20} J/ATP. No known process that converts chemical to mechanical energy does so without some loss to heat. Therefore, due to energy considerations, deriving the torque generated by a stalled cilium or flagellum from fewer than half of the dynein heads is also not possible.

In a moving flagellum, the force-velocity behavior of the dynein dictates that the average force per head decreases with increased velocity. This decrease may be explained by a reduction of the number of dyneins in the duty phase of the crossbridge cycle, or by a reduction in the contribution of force per head. In either case, the reduction in force has been accounted for by the one-quarter reduction in t-force that has already been included in the estimate given above.

An argument could be made that the whole-cell measurements are not sufficient proof that the all of the dyneins must pull to account for the torque produced in a beating flagellum. If the actual torque is less in a beating flagellum we could base our calculations on a reduced total number of contributing dyneins, provided that the work output of each dynein does not exceed the energy available from the hydrolysis of ATP. For instance, it might be reasonable to expect that one dynein head pulls while the next one translocates to a new binding site. The work of Burgess (1995) suggests that the outer arms may work as groups of approximately four pulling and four translocating. Either of these schemes would reduce the number of active bridges by one-half. This would be possible as long as the bending torque was also half of the measured stall value. This would keep the force per dynein head at 5 pN, which is just within energy constraints. In this case, the longitudinal force on the doublets, and likewise the t-force, would be reduced to one-half. Interestingly, the maximum load that the dyneins could support would also drop to one-half of the original calculation. The important thing to note is that any scheme that systematically employs a fixed fraction of the dynein heads will reduce both the t-force and the holding capacity of the dyneins by a commensurate amount, and therefore the original conclusion is still valid. The only difference this would make is that the value of the critical t-force for switching would be reduced proportionately to one-half, or 0.25 nN/μm.

To summarize, it appears that the t-force and summated bearing force of the dyneins both tend to converge to a single value. The one-to-one relationship is improved by the inclusion of dynein force-velocity behavior and differences in inner and outer arm stalling force. Furthermore, it is not altered by the assumption that a fixed fraction of dynein heads participates in force generation. The analysis presented here suggests that the t-force, when switching occurs, is within the range of 0.25–1.0 nN/μm, with 0.5 nN/μm the most likely value.

An estimate from shortened bull sperm

Holcomb-Wygle et al. (1999) obtained the first experimental estimate of the t-force in bull sperm at the switching threshold. In that study, Triton X-100-extracted bull sperm in a reactivating solution containing 1 mM Mg-ATP were shortened by microdissection. Reactivated sperm were selected that had their heads firmly stuck to a glass microscope slide. The flagellum was then shortened by slicing it between

the slide and a stiff glass microprobe. The shortened flagellum can continue to beat when freed from the slide using the microprobe. Bull sperm are large and the axoneme is reinforced with nine outer dense fibers and is enclosed in an elastic sheath. Therefore, the flagellum is much stiffer than the simple flagellum of a sea urchin sperm. When the bull sperm flagellum was shortened to 15 μm, beating stopped. When flagella were shortened to lengths >15 μm but <20 μm, beating continued but was sporadic, characterized by an irregular periodicity and transient arrests. In cells with shortened flagella exhibiting these transient arrests, the curvature was measured at the arrest point.

An arrested flagellum that is near the trigger point for beat reversal is an ideal subject for finding the t-force close to the switch point. In such a flagellum, force-velocity considerations do not apply, as there is no proper motion. The torque balance is greatly simplified, as the viscous drag is equal to zero. The arrest point represents a pure balance of the active torque acting against the structural elastic resistance of the flagellum. If the stiffness is known, then the curvature of the flagellum at the arrest point lets us calculate the internal torque that is bending the flagellum. Once the active torque is known, the linear tension on the doublets that is creating the bending torque can be found by dividing the active torque by the effective diameter of the axoneme. As we have already seen, if we have values for the curvature and linear tension in hand, Eq. 1 allows us to calculate the t-force. A stiffness value of 4×10^{-12} dyne cm^2 was reported by Lindemann et al. (1973), based on flagellar recoil times and the estimated viscous drag acting on flagellum. Holcomb-Wygle et al. (1999) used this stiffness value to determine the internal torque and t-force present in the transiently arrested bull sperm flagella. On this basis, the t-force was estimated to be between 0.15 and 0.2 nN/μm (reported as 0.15–0.2 dyne/cm).

Since that report, Holcomb-Wygle et al. (2001) have directly measured the stiffness of the bull sperm flagellum using force-calibrated glass microprobes. The stiffness of the bull sperm flagellum at the basal portion of the principle piece is 1.0×10^{-11} dyne cm^2, $\sim 2.5\times$ the earlier indirect estimate. Correcting the earlier reported values to reflect the flagellar stiffness obtained by direct measurement yields a t-force at the switch point of 0.4–0.5 nN/μm. It is noteworthy that while this method of estimation depends on the accuracy of the flagellar stiffness, it is completely independent of assumptions about the dynein force per head and number of participating dyneins. Therefore, it contributes a valuable independent confirmation of the t-force magnitude near the switch point.

The switching mechanism

The three lines of evidence examined here all point to the same conclusion: the t-force/μm that develops in a flagellar bend is, to the best approximation, equal to, or greater than, the maximum force the dyneins in one micron of flagellum can sustain. To follow this line of reasoning one step further, it is hard to envision how the dyneins could continue to remain active when subjected to loading greater than they collectively can generate. It is probably not necessary to exceed the mechanical break point of the chemical bond at the attachment site to achieve switching, since the molecular motors exhibit stochastic behavior. It is almost certain that when the dyneins are carrying the full stalling force, a bridge, once released, has a reduced probability of reforming. This will effectively initiate a cascade of bridge release. This is why an intact muscle or an intact flagellum cannot exceed the isometric stalling force even when the sliding velocity is negative. In a bridge model for dynein with stochastic behavior, such as the one proposed by Brokaw (1999b), negative sliding velocities result in progressively decreased force production. Thus, attempting to overload the dyneins results in reduced bearing capacity of the aggregate assembly of motors. Therefore, when t-force meets, or exceeds, the stalling force of the dyneins it should result in switching the dyneins ''off'' and terminating the episode of dynein activity. The mechanism will be a cascade of detachment whereby one dynein releasing stochastically precipitates a cascade of release as the ratio of t-force to adhesive force becomes progressively higher as detachments overtake reattachments.

It is the nature of the dynein molecule that the attachment to the B-subtubule is accomplished through a slender extension of the dynein head called the stalk or B-link (Goodenough and Heuser, 1982). While the details of the force-producing mechanism are still unknown, the force must be communicated to the B-subtubule via the stalk attachments, as these are the sites of the tubulin-binding domain (King, 2000). It is clearly seen in quick-frozen deep-etch replicas of *Tetrahymena* and *Chlamydomonas* axonemes (Goodenough and Heuser, 1982) that the stalks of dynein are slender projections that bridge a relatively large portion of the interdoublet distance. Therefore, the stalks will still define an axis of force transmission as illustrated in Fig. 3. Consequently, there will always be a longitudinal and a transverse component of the tension generated by the dynein bridge.

As the magnitude of the t-force increases at the crest of a bend, the transverse component of the dynein force will increase. If we let the maximum force-bearing capacity of the dynein bridge represent the magnitude of the force vector along the dynein stalk axis then, by the Pythagorean theorem, the transverse component of the dynein-bridge force will converge to the maximal force-bearing capacity as the t-force increases.

The only alternative force-bearing structures present between the doublets are the nexin links. The nexin also bear a fraction of the t-force as indicated in Fig. 3. At the crest of a proximal bend where switching occurs, the shear angle is ≈ 1 radian in a sea urchin sperm. The shear angle is

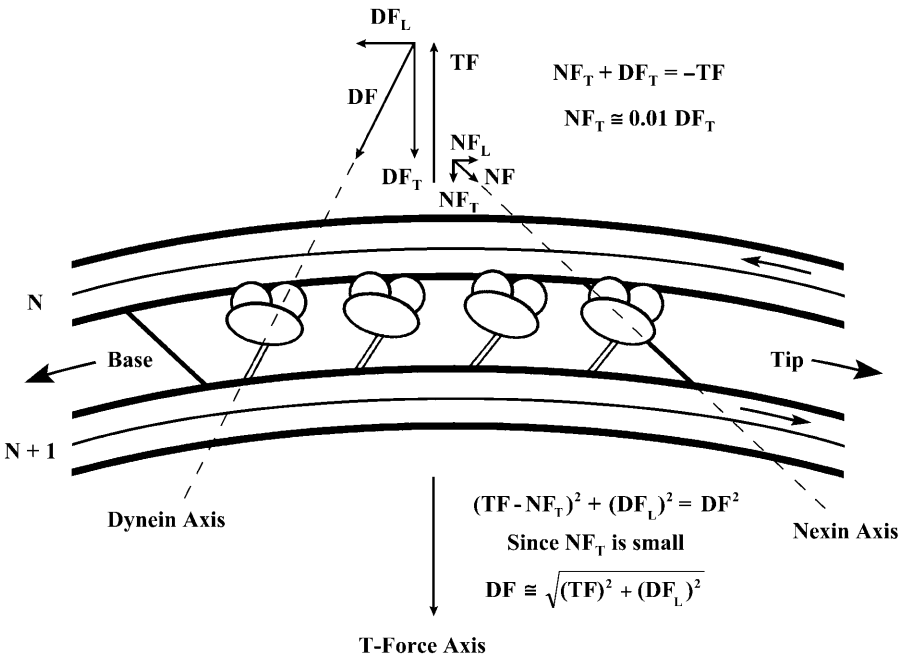

FIGURE 3 The relationship of dynein force to t-force in a flagellar bend. The figure schematically represents two doublets bridged by active dyneins in a region of active bending. The arrows on the doublets indicate the direction of sliding. The dynein force is transmitted from one doublet to the neighboring doublet through the stalks (or B-links), which are slender α-helical extensions of the dynein molecule. The axis of the stalk (*Dynein Axis*) defines the direction of the dynein force (*DF*). The stretched nexin links also contribute an elastic force (*NF*) in the axis defined by the nexin links (*Nexin Axis*). The vector diagram above the schematic breaks down the *DF* and *NF* into the longitudinal (DF_L/NF_L) and transverse (DF_T/NF_T) components. In the vector analysis, the t-force vector (*TF*) is balanced by the DF_T and NF_T vectors . The text provides an analysis of the magnitude of the nexin elastic force. This force component is ~1% of the total t-force magnitude. Therefore, there is a close equivalence between the magnitude of t-force and the transverse component of the dynein force (DF_T), and they are balanced in a Newtonian equilibrium. The relationship of the total dynein force exerted along the dynein stalk to the t-force can therefore be found by application of the Pythagorean theorem, as shown below the schematic.

the angle between a tangent to the flagellar base and a tangent to the flagellum at the point under consideration. The sliding displacement between doublets may be found by multiplying the shear angle, in radians, by the interdoublet distance. Consequently, near the switch point the sliding displacement between doublets is approximately equal to the interdoublet distance. If we take 55 nm as the interdoublet distance for all doublet pairs 2–4 and 7–9, then the stretch of the nexin links can be found using the Pythagorean theorem. If the resting length of the nexin is 30 nm and the lateral sliding displacement is 55 nm, then the nexin must stretch 48 nm. When this stretch is multiplied by 2.0×10^{-5} N/m, the best estimate of the nexin elasticity (Yagi and Kamiya, 1995), the result is a force per nexin of $\approx 1.0 \times 10^{-12}$ N/nexin, of which 4.8×10^{-13} N is transverse to the doublets. The nexin links are spaced at 96-nm intervals. Therefore, the t-force contributed by the nexin links is $\sim 5.0 \times 10^{-12}$ N/μm. This locally produced contribution to the t-force is equal to 1% of the total t-force at the switch point, and for all practical purposes can be ignored.

The local contribution of t-force from the nexin links is small. Thus the force balance between the doublets, up to the point of switching, can be described as a Newtonian balance between the global component of the t-force and the transverse component of the tension on the dynein bridges. As the t-force increases toward equality with the maximum dynein holding force, the fraction of the dynein force directed against the t-force is expected to increase until switching is initiated. This relationship is reflected as a change in the angle of the stalk connectors over the course of the beat cycle.

The work of Kamiya and Okagaki (1986) provides direct experimental support for this idea that the dyneins can generate sufficient t-force to terminate their own action. In that study, paired doublets at the frayed tips of *Chlamydomonas* flagella were observed to undergo bending followed by separation of the interacting pair in the bent region. In essence, this experiment provides the proof of principle that the t-force can terminate the dynein interaction in the manner described here.

DISCUSSION

Gibbons and Gibbons (1973) originally noted that in sea urchin sperm the binding of the dyneins to their attachment sites on the B-subtubule decreases the interdoublet distance. This relationship has also been independently confirmed in cilia (Warner, 1978; Warner and Mitchell, 1978; Zanetti et al., 1979). Mechanically, this is very important. It means that the dynein arms, when they are bound to the B-subtubule, must bear most or all of the t-force acting to pry the doublets apart. This is because the relaxed spacing of the doublets, when only the nexin links and spokes govern the spacing, is greater than the spacing when the dyneins are attached. Consequently, during episodes of dynein activity it is the dyneins that must resist the t-force that acts to pull the

doublets apart, since the other structural elements favor a wider spacing. For this reason, imagining that working dyneins are shielded from the t-force by another structure within the axoneme is not a credible option. Therefore, when the dynein motors are engaged and doing their work, the force balance between the t-force and the total carrying capacity of the dynein arms is a real issue that cannot be ignored.

In a dynein motor protein, the force-producing mechanism is not yet known. However, it is known that the ATP binding domain is on the globular head and the attachment to the B-subtubule is accomplished through the stalk (King, 2000). Transmission of the bridge force through the stalk to the adjacent doublet may be a mechanism to permit force transmission in both the transverse and longitudinal directions. This may account for the rough equivalence between the switching t-force and the maximum isometric force of the dynein motor.

What happens when the dyneins let go?

Once the t-force breaks some of the dynein attachments, then fewer dyneins are left to carry the remaining t-force near the discontinuity. This means that less t-force will be needed to keep the detachment going once it has started, and it can spread distally along the flagellum as the wave propagates. The Geometric Clutch computer model suggests that as little as 1/10 of the initial triggering t-force may suffice for propagation of the wave of dissociation. This predicts that the curvature needed for switching in the proximal part of the flagellum should be greater than the subsequent propagating curvature, and in fact, this is seen in the data presented by Brokaw (1984, 1999a) for sea urchin flagella.

When the active dyneins let go, the t-force must be redistributed to other structures or the axoneme will split. Weakened axonemes do in fact split (Lindemann and Gibbons, 1975; Tamm and Tamm, 1984; Sale, 1986; Satir and Matsuoka, 1989). The first splits are often observed between doublets 2 and 3, 3 and 4, 7 and 8, and 8 and 9 (Tamm and Tamm, 1984; Sale, 1986; Lindemann et al., 1992). Fig. 1 *b* depicts the dyneins releasing between doublets 7–9. When the dyneins release, the nexin links are certainly well-positioned to resist the t-force. These structures bridge the outer doublets at 96-nm intervals in register with the dynein regulatory complex (Stephens, 1970; Dallai et al., 1973; Warner, 1976; Warner et al., 1985; Goodenough and Heuser, 1985). They are elastic structures and have been observed to stretch many times their resting length (Dallai et al., 1973; Warner, 1976; Olsen and Linck, 1977).

Naturally occurring spoke and central-pair deficient flagella, the so-called 9 + 0 flagella, exhibit a low amplitude helical beat but are vigorously motile (Gibbons et al., 1985; Ishijima et al., 1988; Wooley, 1997). Therefore, in these flagella the nexin links and the cell membrane are the only structures positioned to resist the t-force when the dynein arms release. Wooley (1997) provides evidence that the nexin links are effectively normal in the 9 + 0 flagella of eel sperm. Gibbons et al. (1985) report that when the membrane of these sperm is removed by detergent extraction, the flagella can be reactivated but are more fragile than sea urchin sperm and often disintegrate. On the basis of this evidence, the nexin must bear most of the t-force in these flagella.

It is very interesting that all of the naturally occurring 9 + 0 flagella have a helical beat. These flagella completely lack the central pair and spokes. Ishijima et al. (1988) compare sperm from two species of eel, i.e., one with, and one without, the central apparatus. They find that the spokes and central pair impart a planar beat with large amplitude, much like the beat in sea urchin. They suggest that the spoke and central-pair apparatus is the key to planar beating.

The story becomes even more interesting when we examine the work of Brokaw et al. (1982) and Brokaw and Luck (1985) who looked at the effects of the central-pair apparatus on the flagellar beat by selective mutation in *Chlamydomonas*. The spoke head and central-pair deficient mutants do not show a helical beat like the naturally occurring 9 + 0 flagella. Instead, they have a planar beat of large amplitude and beat at a lower frequency than wild-type. Therefore, the role that the spokes and central pair play in determining the plane of the beat is not a simple issue that can be resolved within the context of this report. What is relevant to the present analysis is that both naturally occurring 9 + 0 flagella, and spoke-head or central-pair deficient mutants of *Chlamydomonas*, can beat without disintegration of the axoneme.

Together, these observations provide proof that the nexin links are sufficient to restrain the t-force and allow the flagellum to beat without splitting. The Geometric Clutch computer model predicts (Lindemann and Kanous, 1995) that for simple flagella and cilia the elasticity of a nexin link should lie in the range of $1.0–3.0 \times 10^{-5}$ N/m (0.01–0.03 dyne/cm). Yagi and Kamiya (1995) provide the one estimate of nexin elasticity derived from experimental measurements. Their measurements place the value of the nexin elasticity at 2×10^{-5}N/m (0.02 dyne/cm), consistent with the theoretical value. If the nexin links bear the entire t-force they would be expected to stretch to many times the diameter of the axoneme, as noted in an earlier review (Lindemann and Kanous, 1995). The elastic behavior of the nexin is unlikely to be linear over large distances. More likely, the nexin reaches an elastic limit as do other elastic structures, at which point the elastic coefficient increases dramatically just before the breaking point. However, the nexin must be able to stretch sufficiently to accommodate the normal amount of sliding without reaching the breaking point. In a normal propagating bend of sea urchin the doublets adjacent to the 3-central-pair-8 partition translocate more than 40 nm relative to doublets 3 and 8. Therefore, the axoneme should, at minimum, be able to stretch to double its normal diameter

in the plane of bending when only the nexin links resist the t-force, as illustrated in Fig. 1 *c*.

The helical activation of the doublet pairs in the 9 + 0 sperm would have the effect of distributing the distortion, caused by stretching the nexin links, so that individual doublet pairs will separate one at a time, as each pair is pulled apart individually by the t-force. In these flagella, the number of dynein arms is also reduced (most are outer-arm deficient) and so the t-force is also proportionately less. Therefore, the distortion of the axoneme is effectively minimized. This should not be the case in the spoke-head mutants of *Chlamydomonas*. These flagella exhibit planar bending and the distortion should be large enough to be directly observed. This could conceivably be accomplished with a technique such as bead attachment successfully employed by Brokaw (1991) on sea urchin sperm. It might also be an ideal subject for resolution with the new technique of cryoelectron tomography, which has been shown to be capable of reconstructing the three-dimensional relationship of cytoskeletal elements in vitrified unfixed living cells (Medalia et al., 2002).

A role for the spokes

In an intact axoneme, the spoke apparatus must carry the main share of t-force after the dyneins disengage, as is illustrated in Fig. 1. Much of the t-force will be transmitted to the spoke attachments at the central-pair projections from doublets 1 and 5–6. This is because, as mentioned earlier, the dyneins on each side of the axoneme, when acting together to bend the flagellum, serially transfer the force they generate to the most widely spaced elements, which are doublets 1 and 5–6. The attachment of spokes from doublets 1 and 5–6 to the hub may play an important role in t-force redistribution during the switching event. Fig. 1 incorporates features of the central-pair apparatus taken from the work of Smith and Lefebvre (1997) and Rupp et al. (2001). Spoke number 1 forms a kind of caliper with the cantilever-like structure called the central-pair projection.

The geometry of proteins surrounding the central pair, as summarized in Fig. 1, suggests a possible function in the management of stress within the axoneme. The central-pair projections could buffer the t-force by behaving like pair of rocker arms, literally a biological shock absorber. At the release point in the switching cycle, these projections would flex outward when the t-force is suddenly transferred from the active dyneins to the spoke apparatus, as illustrated in Fig. 1 *b*. This would provide some elastic accommodation for the t-force and would allow the doublets on what was the active side to separate, although still permitting the opposite set of doublets to begin an episode of engagement, as seen in Fig. 1 *b*.

The protection from the strong t-force afforded to the doublets on the opposing side may, in fact, be an important contribution. Without the spokes, the nexin links on both sides of the axoneme will be stretched in the direction of the t-force acting across doublets 1 and 5–6. This will prevent any further dynein bridge engagement, as shown in Fig. 1 *c*. Both sets of dyneins will remain inactive until the t-force subsides sufficiently to allow the doublets on the inactive side to move back together. In the absence of the radial spokes, the collapse of the t-force will only occur as the wave of dissociation spreads nearly to the tip of the flagellum. Consequently, in a spoke-head deficient or spoke-attachment site deficient flagellum, the beat must go all the way to one side of the possible range of motion, and decay, and then repeat the process on the other side. This is because the inhibiting effect of the t-force is felt by the dyneins on both sides of the axoneme. This is very much like the behavior reported by Brokaw and Luck (1985) for a spoke-head defective mutant of *Chlamydomonas*. Although this form of motility is still a coordinated beat, it is not nearly as effective for propulsion as a normal ciliary or flagellar beat. Rapid reciprocation of the dyneins on opposite sides of the axoneme is required for effective propulsion in the wild-type beat pattern.

The cantilever arrangement at the central hub provides some freedom for elastic distortion so that very little of the t-force is carried by the spokes and central-pair apparatus when the dyneins are still attached. Therefore, this arrangement not only prevents the axoneme from experiencing extreme distortion when bridge release occurs, but also insures that the full t-force is available for dynein switching before release occurs.

Transmission electron micrographs show that there are ~30 spokes on a micron of outer doublet in *Tetrahymena* (Warner and Satir, 1974). If we take the t-force at switching to be 0.5 nN/μm, then the spoke and hub force-bearing axis from doublet 1 through the central cantilever to doublet 5–6 will be subjected to this force. The spokes of the adjacent doublets 2, 4, 7, and 9 must also carry some of the total t-force. Since they are not aligned with the axis of the t-force, their contribution would likely be in proportion to the cosine of the angle of their spokes to the axis of the t-force. For spokes 2 and 4, this is cos (40°) or ~75% of the load that spoke 1 would carry. This makes the effective number of spokes 75/μm for the purpose of calculation. Therefore, during the switching transition each spoke of doublet 1 would have to support 7 pN of the total t-force, and the adjacent spokes ~5 pN.

Warner and Satir (1974) have shown convincing evidence that the spokes can translocate, or jump, when sliding subjects them to lateral strain. The dynein-switching event occurs close to the zero shear-rate point of the bending cycle. Consequently, the spokes should not be jumping laterally at this point in the beat cycle and could provide the maximum structural stability. Spoke jumping occurs in the regions where active sliding is taking place, as indicated by the work of Warner and Satir (1974). That would correspond to the interbend regions where t-force is minimal. What kind of

a mechanical connection might be able to translocate laterally and yet, provide as much as 7 pN of resistive force against dissociation? This is within the capability of single molecules of the processive motor protein kinesin as reported by Nishiyama et al. (2002). This is an intriguing possibility, since kinesin has been reported to be associated with the central-pair projections of the central-pair apparatus (Smith and Lefebvre, 1997).

Does this force-based view of the spoke/central-pair apparatus preclude the extensive evidence that the central apparatus and spokes mediate an activation of the motility through a protein kinase based mechanism (Smith and Sale, 1992; Habermacher and Sale, 1995; Porter and Sale, 2000)? The analysis of forces presented here in no sense precludes the presence of biochemical regulators that may turn on, or turn off, the motors or regulate the mechanical attributes of the structure. After all, good motors always have an on/off switch and usually a throttle as well. The point of this analysis is that the forces cannot be ignored. They must be accommodated and accounted for in a working flagellum. Examination of the forces puts some serious constraints on the working mechanism of the system and the mechanical properties of its components.

CONCLUSIONS

The flagellum/cilium is an engine of motility, a true biological machine. Like other engines, the axoneme undergoes a cycle of linked events that harness the release of chemical energy to produce useful work. To understand the internal events in the beat cycle, it is essential that we understand the interaction of the forces from the primary dynein motor proteins with the structural components of the axoneme.

In this report, some of the consequences and predictions that result from a force-based view of the flagellar axoneme have been examined. The analysis supports the idea that the axoneme redistributes force from the dynein motors to create a strong t-force within the bent regions of the flagellum. The magnitude of the t-force appears to be sufficient to play a significant role in terminating the attachments of the dynein motors to the B-subtubule. The crucial point is that the t-force that develops in one micron of a typical beating flagellum is sufficient to overpower the combined force-producing capacity of the dynein in that same segment.

Consistent with this view, the radial spokes and the central-pair projections are subjected to the full magnitude of the t-force during the transition intervals after dynein disengagement, when dynein heads are not engaged on either side of the axoneme. In this capacity, the spokes and central-pair apparatus must manage and redistribute the t-force during switching. This may be especially important in transferring mechanical advantage to the dyneins on the inactive side of the axoneme, by diverting the t-force through the central-pair complex instead of through the interdoublet nexin links. The presence of strong spoke attachments at the central-pair projections will facilitate faster activation of the opposite set of dyneins for rapid beat cycle progression. Release of the spoke-head attachments could delay activation of the opposing dynein set. In this way, the spoke-head attachments at the central-pair projections could modulate the transition between the opposing bridge sets and thus alter the waveform of the beat.

If this prediction is correct, the spoke and central apparatus have a role in the axoneme not previously considered. The spokes attached to the central-pair projections must act as a shock absorber capable of transiently bearing up to 7 pN of force per spoke head during dynein-bridge switching. Yet, the spoke heads of all of the doublets, with the possible exception of 3 and 8, must also have a mechanism of attachment at the central-pair apparatus that allows longitudinal displacement (i.e., spoke jumping, as reported by Warner and Satir, 1974). The best candidate for such a strong but mobile attachment would be through processive motor proteins interacting at each spoke head. In fact, the presence of kinesin-like proteins associated with the central-pair projections has been demonstrated (Smith and Lefebvre, 1997), but not considered within the context of this proposed function.

Ms. Kathleen A. Schmitz-Lesich edited the manuscript, and provided valuable technical expertise in the design and construction of the figures.

This work was supported by grant #MCB0110024 from the National Science Foundation.

REFERENCES

Ashkin, A., K. Shultze, J. M. Dziedzic, U. Euteneur, and M. Schliwa. 1990. Force generation of organelle transport measured *in vivo* by an infrared laser trap. *Nature*. 348:346–348.

Brokaw, C. J. 1965. Non-sinusoidal bending waves of sperm flagella. *J. Exp. Biol.* 43:155–169.

Brokaw, C. J. 1984. Automated methods for estimation of sperm flagellar bending parameters. *Cell Motil.* 4:417–430.

Brokaw, C. J. 1990. The sea urchin spermatozoon. *Bioessays*. 12:449–452.

Brokaw, C. J. 1991. Microtubule sliding in swimming sperm flagella: direct and indirect measurements on sea urchin and tunicate spermatozoa. *J. Cell Biol.* 114:1201–1215.

Brokaw, C. J. 1994. Control of flagellar bending: a new agenda based on dynein diversity. *Cell Motil. Cytoskeleton*. 28:199–204.

Brokaw, C. J. 1999a. Bending patterns of ATP-reactivated sea urchin sperm flagella following high salt extraction of removal of outer dynein arms. *Cell Motil. Cytoskeleton*. 42:125–133.

Brokaw, C. J. 1999b. Computer simulation of flagellar movement: VII. Conventional but functionally different cross-bridge models for inner and outer arm dyneins can explain the effects of outer arm removal. *Cell Motil. Cytoskeleton*. 42:134–148.

Brokaw, C. J., and R. Kamiya. 1987. Bending patterns of *Chlamydomonas* flagella: IV. Mutants with defects in inner and outer dynein arms indicate differences in dynein arm function. *Cell Motil. Cytoskeleton*. 8:68–75.

Brokaw, C. J., and D. J. L. Luck. 1985. Bending patterns of *Chlamydomonas* flagella: III. A radial spoke head deficient mutant and a central pair deficient mutant. *Cell Motil.* 5:195–208.

Brokaw, C. J., D. J. L. Luck, and B. Huang. 1982. Analysis of the movement of *Chlamydomonas* flagella: the function of the radial-spoke system is revealed by comparison of wild-type and mutant flagella. *J. Cell Biol.* 92:722–732.

Burgess, S. A. 1995. Rigor and relaxed outer dynein arms in replicas of cryofixed motile flagella. *J. Mol. Biol.* 250:52–63.

Dallai, R., F. Bernini, and F. Giusti. 1973. Interdoublet connections in the sperm flagellar complex of *Sciara*. *J. Submicrosc. Cytol.* 5:137–145.

Gibbons, B. H., and I. R. Gibbons. 1972. Flagellar movement and adenosine triphosphatase activity in sea urchin sperm extracted with Triton X-100. *J. Cell Biol.* 54:75–97.

Gibbons, B. H., and I. R. Gibbons. 1973. The effect of partial extraction of dynein arms on the movement of reactivated sea urchin sperm. *J. Cell Sci.* 13:337–357.

Gibbons, B. H., B. Baccetti, and I. R. Gibbons. 1985. Live and reactivated motility in the 9 + 0 flagellum of *Anguilla* sperm. *Cell Motil.* 5:333–350.

Goodenough, U. W., and J. E. Heuser. 1982. Substructure of the outer dynein arm. *J. Cell Biol.* 95:798–815.

Goodenough, U. W., and J. E. Heuser. 1985. Substructure of inner dynein arms, radial spokes and the central pair/projection complex of cilia and flagella. *J. Cell Biol.* 100:2008–2018.

Habermacher, G., and W. S. Sale. 1995. Regulation of dynein-driven microtubule sliding by an axonemal kinase and phosphatase in *Chlamydomonas* flagella. *Cell Motil. Cytoskeleton.* 32:106–109.

Hirakawa, E., H. Higuchi, and Y. Y. Toyoshima. 2000. Processive movement of single 22S dynein molecules occurs only at low ATP concentrations. *Proc. Natl. Acad. Sci. USA.* 97:2533–2537.

Holcomb-Wygle, D. L., K. A. Schmitz, and C. B. Lindemann. 1999. Flagellar arrest behavior predicted by the Geometric Clutch model is confirmed experimentally by micromanipulation experiments on reactivated bull sperm. *Cell Motil. Cytoskeleton.* 44:177–189.

Holcomb-Wygle, D. L., K. A. Schmitz, and C. B. Lindemann. 2001. Measurement of the passive stiffness of bull sperm flagella using force-calibrated glass microprobes. *Biophys. J.* 80:71a.

Ishijima, S., K. Sekiguchi, and Y. Hiramoto. 1988. Comparative study of beat patterns of American and Asian horseshoe crab sperm: evidence for a role of the central pair complex in forming planar waveforms in flagella. *Cell Motil. Cytoskeleton.* 9:264–270.

Kamimura, S., and K. Takahashi. 1981. Direct measurement of the force of microtubule sliding in flagella. *Nature.* 293:566–568.

Kamiya, R., and T. Okagaki. 1986. Cyclical bending of two outer-doublet microtubules in frayed axonemes of *Chlamydomonas*. *Cell Motil. Cytoskeleton.* 6:580–585.

King, S. M. 2000. AAA domains and organization of the dynein motor unit. *J. Cell Sci.* 113:2521–2526.

Lindemann, C. B. 1994a. A Geometric Clutch hypothesis to explain oscillations of the axoneme of cilia and flagella. *J. Theor. Biol.* 168:175–189.

Lindemann, C. B. 1994b. A model of flagellar and ciliary functioning which uses the forces transverse to the axoneme as the regulator of dynein activation. *Cell Motil. Cytoskeleton.* 29:141–154.

Lindemann, C. B. 1996. The functional significance of the outer dense fibers of mammalian sperm examined by computer simulations with the Geometric Clutch model. *Cell Motil. Cytoskeleton.* 34:258–270.

Lindemann, C. B. 2002. Geometric Clutch Model version 3: the role of the inner and outer arm dyneins in the ciliary beat. *Cell Motil. Cytoskeleton.* 52:242–254.

Lindemann, C. B., and I. R. Gibbons. 1975. Adenosine triphosphate-induced motility and sliding of filaments in mammalian sperm extracted with Triton X-100. *J. Cell Biol.* 65:147–162.

Lindemann, C. B., and K. S. Kanous. 1995. ''Geometric Clutch'' hypothesis of axonemal function: key issues and testable predictions. *Cell Motil. Cytoskeleton.* 31:1–8.

Lindemann, C. B., and K. S. Kanous. 1997. A model for flagellar motility. *Int. Rev. Cytol.* 173:1–72.

Lindemann, C. B., A. Orlando, and K. S. Kanous. 1992. The flagellar beat of rat sperm is organized by the interaction of two functionally distinct populations of dynein bridges with a stable central axonemal partition. *J. Cell Sci.* 102:249–260.

Lindemann, C. B., W. G. Rudd, and R. Rikmenspoel. 1973. The stiffness of the flagella of impaled bull sperm. *Biophys. J.* 13:437–448.

Medalia, O., I. Weber, A. S. Frangakis, D. Nicastro, G. Gerisch, and W. Baumeister. 2002. Macromolecular architecture in eukaryotic cells visualized by cryoelectron tomography. *Science.* 298:1209–1213.

Nishiyama, M., H. Higuchi, and T. Yanagida. 2002. Chemomechanical coupling of the forward and backward steps of single kinesin molecules. *Nat. Cell Biol.* 4:790–797.

Oiwa, K., and K. Takahashi. 1988. The force-velocity relationship for microtubule sliding in demembranated sperm flagella of the sea urchin. *Cell Struct. Funct.* 13:193–205.

Olsen, G. E., and R. W. Linck. 1977. Observations of the structural components of flagellar axonemes and central pair microtubules from rat sperm. *J. Ultrastruct. Res.* 61:21–43.

Piperno, G., and D. Luck. 1982. Outer and inner arm dyneins from flagella of *Chlamydomonas reinhardtii*. *Prog. Clin. Biol. Res.* 80:95–99.

Porter, M. E., and W. S. Sale. 2000. The 9 + 2 axoneme anchors multiple inner arm dyneins and a network of kinases and phosphatases that control motility. *J. Cell Biol.* 151:F37–F42.

Rupp, G., E. O'Toole, and M. E. Porter. 2001. The *Chlamydomonas PF6* locus encodes a large alanine/proline-rich polypeptide that is required for assembly of a central pair projection and regulates flagellar motility. *Mol. Biol. Cell.* 12:739–751.

Sakakibara, H., H. Kojima, Y. Sakai, E. Katayama, and K. Oiwa. 1999. Inner-arm dynein C of *Chlamydomonas* flagella is a single-headed processive motor. *Nature.* 400:586–590.

Sale, W. S. 1986. The axonemal axis and Ca^{2+}-induced asymmetry of active microtubule sliding in sea urchin sperm tails. *J. Cell Biol.* 102:2042–2050.

Sale, W. S., and P. Satir. 1977. Direction of active sliding of microtubules in *Tetrahymena* cilia. *Proc. Natl. Acad. Sci. USA.* 74:2045–2049.

Satir, P. 1979. Basis of flagellar motility in spermatozoa: current status. *In* The Spermatozoon. D. W. Fawcett and J. M. Bedford, editors. Urban and Schwarzenberg, Baltimore-Munich. pp.81–90.

Satir, P., and T. Matsuoka. 1989. Splitting the ciliary axoneme: implications for a ''switch-point'' model of dynein arm activity in ciliary motion. *Cell Motil. Cytoskeleton.* 14:345–358.

Schmitz, K. A., D. L. Holcomb-Wygle, D. J. Oberski, and C. B. Lindemann. 2000. Measurement of the force produced by an intact bull sperm flagellum in isometric arrest and estimation of the dynein stall force. *Biophys. J.* 79:468–478.

Shingyoji, C., H. Higuchi, M. Yoshimura, E. Katayama, and T. Yanagida. 1998. Dynein arms are oscillating force generators. *Nature.* 393:711–714.

Smith, E. F., and P. A. Lefebvre. 1997. The role of the central apparatus components in flagellar motility and microtubule assembly. *Cell Motil. Cytoskeleton.* 38:1–18.

Smith, E. F., and W. S. Sale. 1992. Regulation of dynein-driven microtubule sliding by the radial spokes in flagella. *Science.* 257:1557–1559.

Stephens, R. E. 1970. Isolation of nexin—the linkage protein responsible for maintenance of the ninefold configuration of flagella axonemes. *Biol. Bull.* 139:438.

Tamm, S. L., and S. Tamm. 1984. Alternate patterns of doublet microtubule sliding in ATP-disintegrated macrocilia of the ctenophore *Beroe*. *J. Cell Biol.* 99:1364–1371.

Warner, F. D. 1976. Ciliary inter-microtubule bridges. *J. Cell Sci.* 20:101–114.

Warner, F. D. 1978. Cation-induced attachment of ciliary dynein cross-bridges. *J. Cell Biol.* 77:R19–R26.

Warner, F. D., and D. R. Mitchell. 1978. Structural conformation of ciliary dynein arms and the generation of sliding forces in *Tetrahymena* cilia. *J. Cell Biol.* 76:261–277.

Warner, F. D., and P. Satir. 1974. The structural basis of ciliary bend formation. Radial spoke positional changes accompanying microtubule sliding. *J. Cell Biol.* 63:35–63.

Warner, F. D., J. G. Perreault, and G. Sander. 1985. Re-binding of *Tetrahymena* 13S and 21S dynein ATPases to extracted doublet microtubules. The inner row and outer row dynein arms. *J. Cell Sci.* 77:263–287.

Wooley, D. M. 1997. Studies on the eel sperm flagellum 1. The structure of the inner dynein arm complex. *J. Cell Sci.* 110:85–94.

Yagi, T., and R. Kamiya. 1995. Novel mode of hyper-oscillation in the paralyzed axoneme of a *Chlamydomonas* mutant lacking the central-pair microtubules. *Cell Motil. Cytoskeleton.* 31:207–214.

Yoneda, M. 1960. Force exerted by a single cilium of *Mytilus edulis*. I. *J. Exp. Biol.* 37:461–468.

Zanetti, N. C., D. R. Mitchell, and F. D. Warner. 1979. Effects of divalent cations on dynein cross bridging and ciliary microtubule sliding. *J. Cell Biol.* 80:573–588.